Proceedings of ASME Turbo Expo 2011
GT2011
June 6-10, 2011, Vancouver, British Columbia, Canada

GT2011-46210

ON-LINE COMPRESSOR CASCADE WASHING FOR GAS TURBINE PERFORMANCE INVESTIGATION

Uyioghosa Igie **Pericles Pilidis** **Dimitrios Fouflias** **Ken Ramsden**

Gas Turbine Engineering
Cranfield University
Cranfield, Bedfordshire
MK43 0AL England

Paul Lambart
R-MC Power Recovery Ltd
6 Stamford Business Park,
Ryhall Road
Stamford, Lincolnshire
PE91XT England

ABSTRACT

On-line compressor washing for industrial gas turbine application is a promising method of mitigating the effects of compressor fouling degradation; however there are still few studies from actual engine experience that are inconclusive. In some cases the authors attribute this uncertainty as a result of other existing forms of degradation. The experimental approach applied here is one of the first of its kind, employing on-line washing on a compressor cascade and then relating the characteristics to a three-dimensional axial flow compressor. The overall performance of a 226MW engine model for the different cases of a clean, fouled and washed engine is obtained based on the changing compressor behavior.

Investigating the effects of fouling on the clean engine exposed to blade roughness of 102µm caused 8.7% reduction in power at design point. This is equivalent, typically to 12 months degradation in fouling conditions. Decreases in mass flow, compressor efficiency, pressure ratio and unattainable design point speed are also observed. An optimistic recovery of 50% of the lost power is obtained after washing which lasts up to 10mins. Similarly, a recovery of all the key parameters is achieved.

The study provides an insight into compressor cascade blade washing, which facilitates a reliable estimation of compressor overall efficiency penalties based on well established assumptions. Adopting Howell's theory as well as constant polytropic efficiency, a general understanding of turbomachinery would judge that 50% of lost power recovered is likely to be the high end of what is achievable for the existing high pressure wash. This investigation highlights the obvious benefits of power recovery with on-line washing and the potential to maintain optimum engine performance with frequent washes. Clearly, the greatest benefits accrue when the washing process is initiated immediately following overhaul.

INTRODUCTION

The occurrence of particulate fouling of the compressor in heavy duty and aero-derivative gas turbine engines has brought about the desirability of compressor washing. Such a measure is of growing interest due to increasing demand for power generation in often remote areas of Alaska, Athabasca, the Niger Delta and the North Sea. Heavy duty engines are widely used for electric power generation and the aero-derivative engines have found application in pumping for oil and gas transmission pipelines, which include gas pressure boosting at variable distances along the network. The application also extends to off-shore and naval propulsion where the deposition of salt particles on the compressor may be prevalent. This arises from sea salt water evaporation.

More specifically, compressor fouling is the deposition and accretion of air-borne particles on compressor blades. This leads to an alteration in the aerodynamic shape of the compressor blade and increases the surface roughness that results in a reduction of the effective blade-to-blade pitch distance. The consequence of this is a reduced mass flow and pressure ratio that consequently reduces power output and thermal efficiency. A recovery of the lost power and efficiency through an increased fuel burn leads to the possibility of elevated exhaust gas temperatures that risk infringing OEM warranties. The reduction of turbine blade creep life due to prolonged high firing temperature is a detrimental effect as well as the increased NOx emission that is accompanied [1].

The philosophy behind on-line compressor washing is that it is a proactive strategy to eradicate the build up of particles on the compressor blades; thereby maintaining performance close to optimum through regular washing. Other major advantages of this method as opposed to the off-line washing, is that it is applicable to full and part-load real time operations and ensures that the stipulated major overhaul interval is maintained, avoiding early shut-downs. These features make it a viable economic approach, as well as a favorable technical-performance objective.

Two gas turbine engines within the vicinity of a busy motorway, around a chemical and food processing industry were investigated in Stalder [2]. This study reports the most beneficial on-line wash regime to mitigate fouling in the engines was 120 hours interval, compared to 700 and 350 hours. This operation coupled with off-line washing extrapolated to 8000 operating hours for one of the 30MW gas turbine amounted to a recovery worth US $450,000 per annum (excluding the operational and maintenance cost). Contrary to previous findings, Syverud and Bakken [3] present an inconclusive account on the benefit of on-line washing at peak load for a compressor driver in an oil field. This two-year investigation for 5 different combinations of wash frequency and cleaning fluid showed no significant improvement in performance. The authors imply that the engine control limits may be a factor affecting trend but did not rule out the role of instrument resolution and repeatability in condition trending. A number of other studies such as Boyce and Gonzalez [4] and Thames et al [5] observe the positive benefits of on-line compressor washing, however it is imperative to bring what may be considered a conjecture, closer to fact.

The method introduced in this study involves the use of a compressor cascade for fouling and washing, which replicates fouled and washed compressor stage characteristics. The major benefit of this approach in relation to studies based on actual engine data is that effects of natural wear and tear over time are almost non-existent here. This is crucial as such unavoidable losses can mimic or exaggerate fouling effect. Thus this approach provides the possibility to better quantify the performance enhancement of on-line washing.

EXPERIMENTAL SETUP

The compressor cascade facility under investigation is a suction-type wind tunnel, with an inlet cross-sectional area of $0.0043m^2$ and mass flow of 5kg/s. This corresponds to an inlet Mach number of 0.3 and Reynolds number of $3.8 \times 10^{5.}$ There are 9 NACA 65-series blades with a chord length of 60mm and span length of 180mm, all placed at a zero design incidence angle for maximum static pressure rise. With an aspect ratio of 3 and number of blades employed, this specification conforms to a requirement for obtaining good two-dimensionality of the flow as highlighted in Dixon [6] and Pollard and Gostelow [7]. The concern about such a design consideration arises from the reduction in static pressure due to boundary layer growth.

Figure 1 illustrates the cascade setup, for which upstream pressure measurement is acquired using a pitot-static tube whilst downstream a three-hole cobra probe is used. The measurements at these stations are along a traverse line one-chord distance from the leading and trailing edge as depicted in Figure 2. Taking measurements at the specified chord distance is a generally acceptable convention in analysing two-dimensional cascade flows especially downstream. This is because sufficient mixing of the flow downstream has occurred [8]. Figure 2 also indicates a reference point marked 0mm along the traverse. This point is considered at the trailing passage between blade 4 and 5. Such approach is taken into account for convenience, nulling the three-hole probe in a relatively steady region rather than the trailing wake of blade 5 (the cascade middle blade). Markings -40mm and 120mm indicate the range of traverse distance covered for the three middle blades with respect to the reference point.

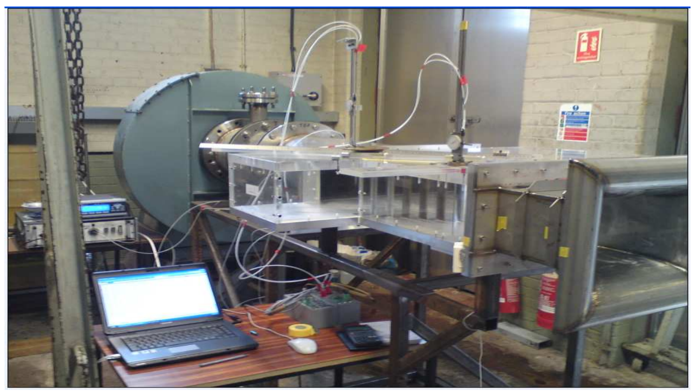

Figure 1 The compressor cascade setup

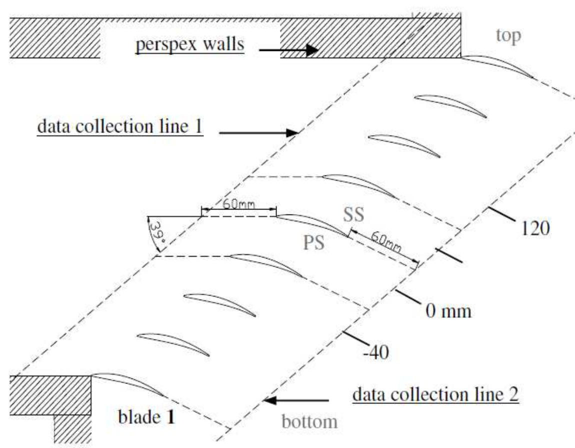

Figure 2 Upstream and downstream traverse measurement locations

FOULING PARTICLE ROUGHNESS AND EFFECTS

The roughness of compressor blades as stated is influenced by the deposition of airborne particles, which leads to a higher surface roughness over time. A realistic case of employing high capture efficiency filters ensures that particle sizes above 0.2µm can be collected. However, high capture efficiency is not always attainable throughout a range of particle sizes between 0.2µm to 100µm [9]. With lower capture efficiencies at microscopic and some sub-micron diameter, particle fouling still remains a threat. In fact aerosol sea salt can gain access into compressor through salt leaching under high ambient humidity [1] which may eventually increase in size when dry [10].

In this study, carborundum particles are applied uniformly on the blade, after the initial application of a thin layer of liquid grease as the sticky agent. The roughness of the particles as provided by the supplier is 102µm, which is equivalent to a roughness height-to-chord *k/c* of 0.0017. The choice of particle roughness height relates to the diameter of salt particles which could be found in an actual engine. However this would depend on the environment and rate of particle accretion on the blades. Figure 3 indicates the three-middle roughened or fouled blades investigated. An examination of the clean (smooth) case for the same blades is included in Figure 4.

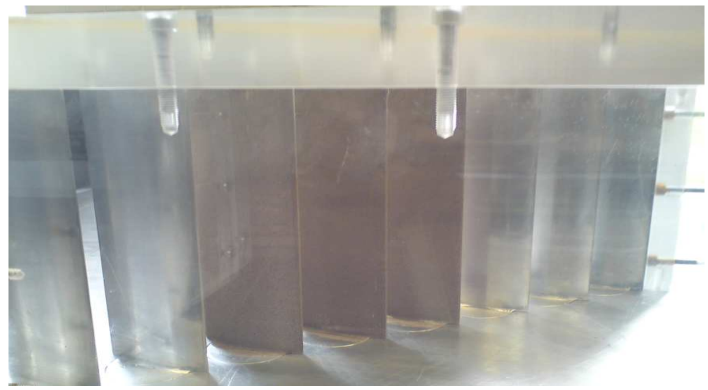

Figure 3 Roughened middle blades in the cascade

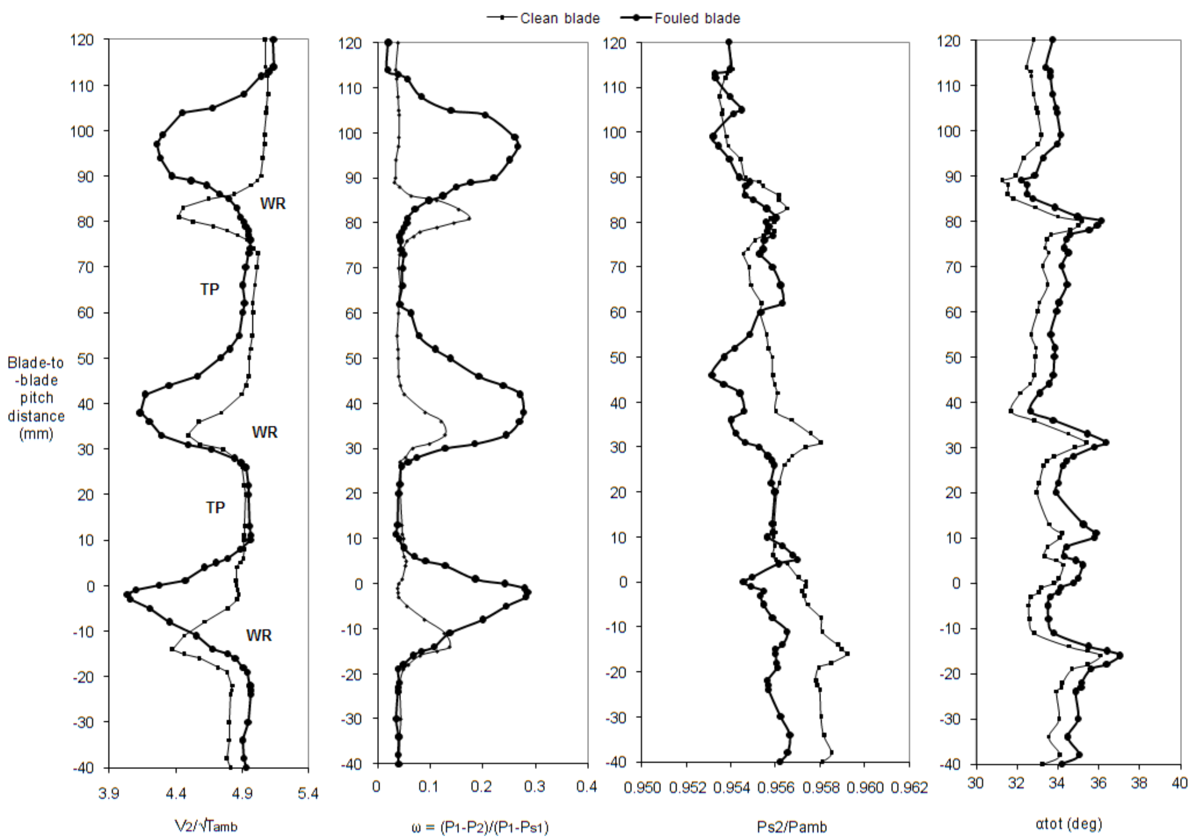

Figure 4 Downstream non-dimensional velocity, total pressure loss coefficient, non-dimensional static pressure and exit flow angle for a clean and fouled blade

At downstream station along the y-axis traverse, the non-dimensional velocity, total pressure loss coefficient, non-dimensional static pressure and the exit flow angle for the smooth and fouled blade is provided in Figure 4 above. The impact of noise has been reduced in the original data using moving averages. The average error relative to the actual data for the clean and fouled blade is 0.05% and 0.09% respectively. The plot of non-dimensional velocity for the smooth blades indicates a higher velocity along the trailing passage (TP) or pitch, when compared with the wake region (WR).The profile of the latter is normally expected to diminish farther downstream due to mixing. This is also depicted in the 3D numerical model contour plot of velocity in Figure 5.

For the fouled blade in Figure 4, there is a general increment in non-dimensional velocity along the passage and a reduction in the effective blade pitch. This can be attributed to boundary layer thickening where the blade profile total pressure loss coefficient increases for the rough blades, in the wake region. As expected, the plot of average non-dimensional static pressure indicates a mean reduction for the fouled blade. This is a consequence of the reduced passage and velocity increment (thereby acting against the cascade diffusing effect highlighted in the smooth blade). The increase in velocity also leads to a more turbulent flow, giving rise to higher exit flow angles presented in the last of the plots.

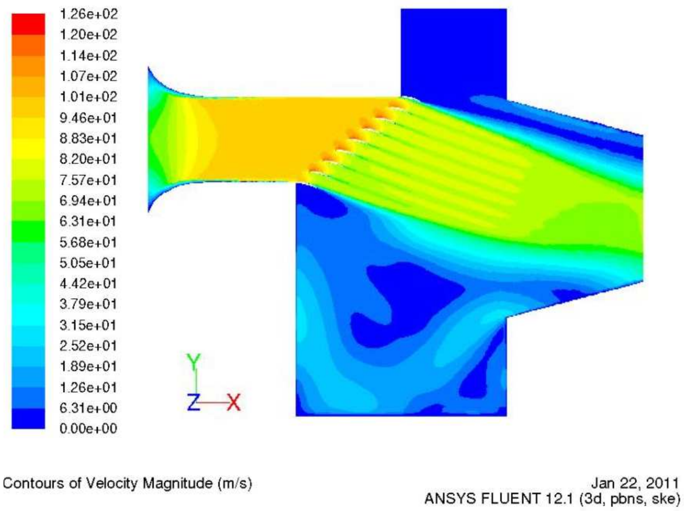

Figure 5 Contours of velocity, indicating wake diminishing profile with velocity increase due to mixing between higher passage velocities

CASCADE COMPRESSOR WASHING

For washing of the cascade blades, R-MC demineralised water concentrate has been mixed with water in the ratio of 1:4, amounting to a density of 992 kg/m^3 when heated to 50^{o}C. The injection pressure is 90bar, whilst the nozzle diameter and area is 0.51mm and 0.08mm^2 respectively. With air inlet mass flow of 5kg/s, the stated conditions yield a wash fluid-to-air ratio of 0.002. This is consistent with the acceptable levels found in many high pressure industrial applications investigated in Mund [11]. Figure 6 shows the position of the flat spray nozzle (at mid-plane) employed at the inlet of the cascade tunnel. Under the current high pressure conditions, the spray angle droplet diameter range is between 50 and 150µm.

Figure 6 Flat spray nozzle fluid injection

After the first 5 minutes of washing, there was a visible removal of particles from the blade leading edge, that improved imperceptibly up to an additional 5minutes of wash as indicated in Figures 7 and 8.

Figure 7 Washed middle blades after 5mins

Figure 8 Washed middle blades after first 10mins

The additional plot of non-dimensional velocity and total pressure loss coefficient for washed blade is presented in Figure 9. For the washed blade, this figure indicates a shift in the wake region towards the clean blade (between traverse locations -20mm and +20mm). A similar trend is observed between locations +80mm and +120mm. This signifies an opening of the passage that often leads to an increase in static pressure. The blade profile total pressure loss coefficient also validates this finding, indicating a slight reduction of the losses. An average error of 0.03% is obtained after reducing the scatter in the data for the washed blade.

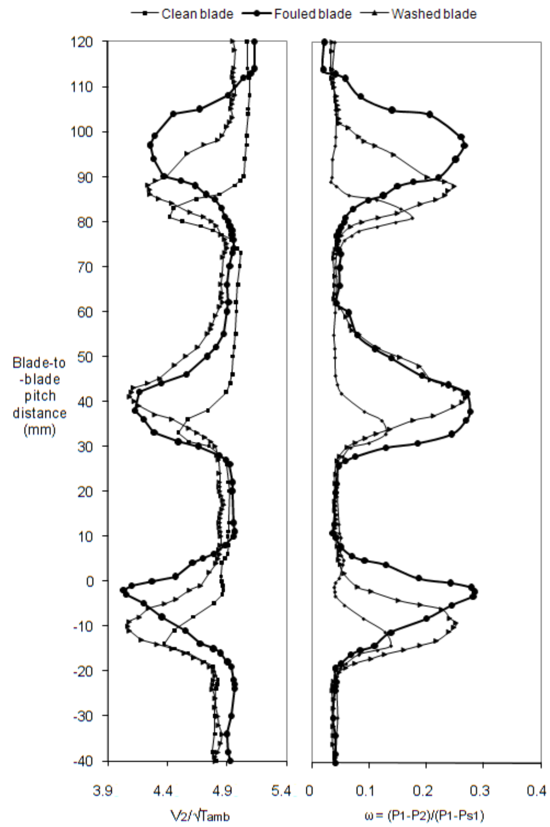

Figure 9 Downstream non-dimensional velocity and total pressure loss coefficient for clean, fouled and washed blade

CORRECTING CASCADE CHARACTERISTICS TO ACHIEVE MEAN STAGE COMPRESSOR CONDITIONS

The complex and anisotropic nature of flow conditions in a compressor stage makes it difficult to predict the actual stage performance in relation to their design objective. As a result, compressor cascade data are useful in predicting and providing an understanding of the potential flow.

Howell [12] proposed the use of two-dimensional cascade data together with theoretical considerations to account for mean stage performance of an actual compressor. To achieve this, correction factors relating to stage losses are applied to cascade performance to produce typical stage flow characteristics. These effects were observed as two trailing vortices downstream of the blade. Howell adds that this is often a combination of tip and axial clearance effect, annulus wall boundary layer and wakes from preceding blade row. To obtain actual data for these corrections, an extensive test on a full scale multi-stage and single stage fan was investigated. This involved traversing around the compressor periphery, which led to categorising loss, as highlighted in Figure 10. The figure also shows the variation of stage efficiency for different flow coefficients.

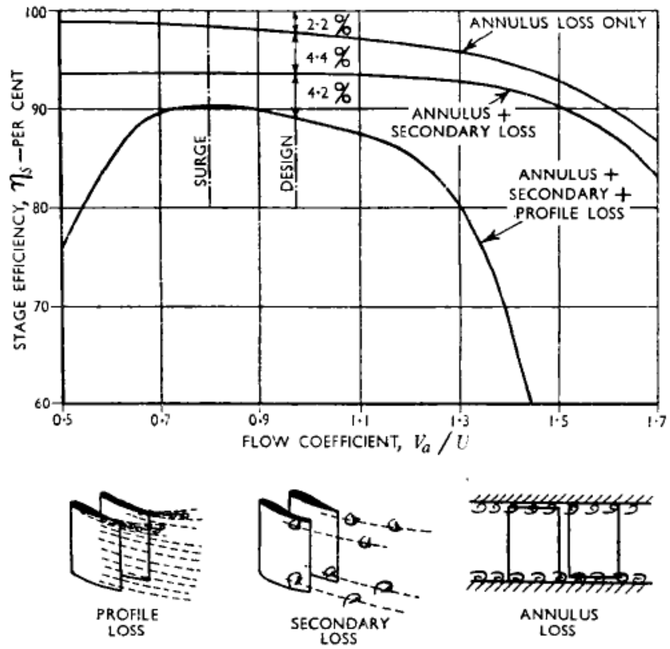

Figure 10 Three-dimensional loses in an axial compressor stage [12]

Profile loss arises from blade skin friction which is obtained from cascade experiments. The profile drag coefficient is then calculated from

$$C_{Dp} = \frac{s}{c}\left(\frac{\Delta P_s}{1/2\rho V_1^2}\right)\frac{\cos^3 \alpha_m}{\cos^2 \alpha_1} \qquad (1)$$

Stage annulus loss accounts for wall friction as shown in Figure 10. This figure indicates that for a compressor with 90% stage efficiency, approximately 2% of its loss is due to annulus effect. Howell’s study propose an estimate for annulus wall drag coefficient as

$$C_{Da} = 0.02\frac{s}{h} \qquad (2)$$

Trailing vortices, viscous dissipation of induced resultant velocities as well as other three-dimensional separation in the flow constitutes secondary loss [12, 13]. The figure also indicates approximately 4% loss is contributed by secondary effects and a similar proportion from the profile loss. Secondary drag coefficient is estimated as

$$C_{Ds} = 0.018 C_L^2 \qquad (3)$$

C_L is the lift coefficient derived as

$$C_L = 2\frac{s}{c}\cos\alpha_m(\tan\alpha_1 - \tan\alpha_2) - C_D\tan\alpha_m \quad (4)$$

where

$$\tan\alpha_m = 0.5(\tan\alpha_1 + \tan\alpha_2) \quad (5)$$

The overall drag coefficient for the stage is then calculated summing up equation (1), (2) and (3) highlighted in the equation below.

$$C_D = C_{Dp} + C_{Da} + C_{Ds} \quad (6)$$

In a compressor stage, the axial velocity at mid-section is known to be greater than mean stage velocity due to the annulus wall boundary layer discussed previously. Howell's study identifies this effect that increases until the fourth stage, after which there is little further increase. This means that for each individual stage, the actual work done is below the intended design requirement. However this study also points out the theoretical compensating increase in the work done towards the tip and hub due to a reduced velocity. Further to that, it concludes that stalling at these ends mitigates such an increase in work done.

A correction known as the work done factor (λ) of approximately 0.86 is proposed as the mean value for multi-stage compressors in Howell's study. Horlock [13] states that some studies have considered a factor of 0.96 at the entry where the annulus boundary layer is relatively thin, though the value is reduced progressively to 0.85 at rare stages. In a later study, Howell and Bonham [14] provide mean work done factors for axial compressors depending on the number of stages.

Applying theses corrections to cascade data, with an assumption of 50% stage reaction in Howell's study, the results where validated against actual stage performance such as the temperature rise coefficient

$$\frac{c_p\Delta T_s}{0.5U^2} = 2\lambda\left(\frac{V_a}{U}\right)(\tan\alpha_1 - \tan\alpha_2) \quad (7)$$

stage or polytropic efficiency;

$$\eta_p = 1 - \left\{\frac{2}{\sin(2\alpha_m)} \times \frac{C_D}{C_L}\right\} \quad (8)$$

and pressure rise coefficient;

$$\frac{\Delta P_s}{0.5\rho U^2} = \eta_p\left(\frac{c_p\Delta T_s}{0.5U^2}\right) \quad (9)$$

Figure 11 below indicates the performance for both cases plotted against the flow coefficient. The plots indicate a good relationship between the cascade-to-stage correlated results and that of the actual stage.

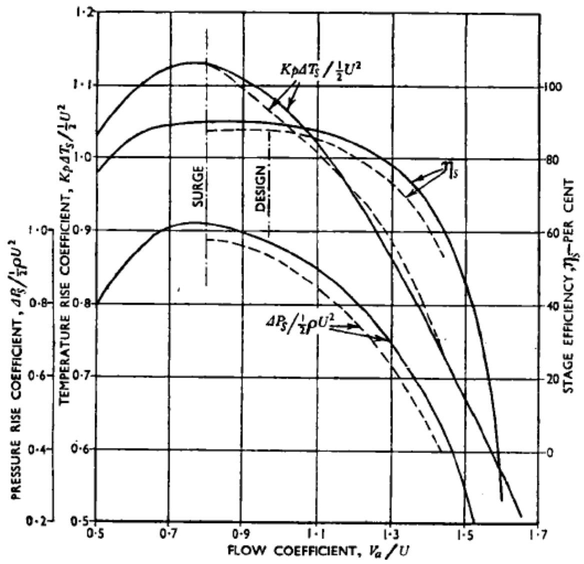

Figure 11 Stage efficiencies versus flow coefficient for the cascade-to-stage and actual stage [12].

In this present study, the same procedure is followed, using the cascade performance data for a theoretical stage velocity triangle with 50% reaction. This means half the increase in static pressure rise in the stage is contributed by the rotor. In other words, the rotor outlet flow angle (α_2) is equal to that of the stator (α_4). Similarly, the rotor inlet flow angle (α_1) is equal to the stator inlet flow angle (α_3) as explained with Figure 12.

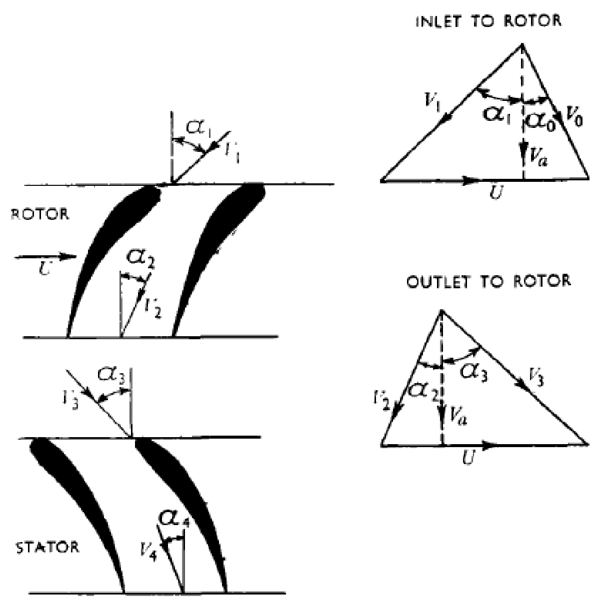

Figure 12 Velocity triangles for a compressor stage [12]

The ratio of axial velocity to rotational speed known as flow coefficient (ϕ) is then derived from

$$\frac{U}{V_a} = (\tan\alpha_1 + \tan\alpha_2) = (\tan\alpha_2 + \tan\alpha_3) \quad (10)$$

$$\left(\frac{U}{V_a}\right)^{-1} = \phi = \frac{1}{(\tan\alpha_1 + \tan\alpha_2)} \quad (11)$$

The stage loading coefficient becomes

$$\psi = \frac{\Delta H}{U^2} = \lambda\phi(\tan\alpha_1 - \tan\alpha_2) \quad (12)$$

After the previous preliminary consideration, a mean work done factor (λ) of 0.85 applicable to a 17 stage compressor [14] is adopted. The number of stages corresponds to a typical pressure ratio of 16.6 considered in the engine model of the next section. Using the correction factors, the polytropic efficiency is calculated to be 90.4% for the clean blades. Similar calculations for the fouled and washed blades has been conducted and provided in Table 1. Such off-design values were obtained from the changes in the cascade blade profile drag in equation (1).

To estimate the overall efficiency of the compressor, constant polytropic efficiency has been assumed for the successive number of stages. With the stated pressure ratio, the isentropic efficiency according to equation (13) is 86%. The same calculation for fouled and washed blades is conducted, arriving at their respective polytropic efficiencies. Table 1 indicates the individual isentropic efficiencies and the relative percentage decrease and increase.

$$\eta_c = \frac{PR^{\left(\frac{\gamma-1}{\gamma}\right)} - 1}{PR^{\left(\frac{\gamma-1}{\gamma\eta_p}\right)} - 1} = 86\% \quad (13)$$

Table 1 Polytropic and isentropic efficiency for clean, fouled and washed blade

	Polytropic Efficiency	*Isentropic Efficiency*	***Isentropic Efficiency Reduction/Increase***
Clean blade	90.4%	86.0%	0.0%
Fouled blade	86.4%	80.3%	6.6% ↓
Washed blade	88.0%	83.0%	3.4% ↑

Mass flow between the three middle blades has been taken during the experiment, with each passage contributing one-third of the total mass flow. The non-dimensional form is adopted to compare the different cases. Table 2 indicates the non-dimensional mass flow percentage reduction for a fouled blade and the percentage gain due to washing.

Table 2 Non-dimensional mass flow penalty and recovery for a fouled and washed blade

	Non-Dimensional Mass Flow Reduction/ Increase
Clean blade	0.0%
Fouled blade	0.69% ↓
Washed blade	0.44% ↑

GAS TURBINE PERFORMANCE

The overall engine performance due to compressor fouling and washing, in relation to a clean engine is investigated. In-house performance simulation software (TURBOMATCH) is employed to calculate the engine design condition with clean blade isentropic efficiency (see equation 13) at the stated pressure ratio.

Off-design performance calculation due to fouling and washing is derived based on compressor map scaling from the design point. This also involves mass and energy balance in the engine model, which is achieved through iterations to match the engine components. To obtain these new engine conditions, the input variables of percentage change in isentropic efficiency ($\Delta\eta_c$%) and non-dimensional mass flow (ΔW%) are included in the design model. This operation is achieved using the following relations [15] below.

$$\eta_{c(new)} = (1 - \Delta\eta_c\%) \times ETASF \times \eta_{cMap} \quad (14)$$

$$W_{(new)} = (1 - \Delta W\%) \times WASF \times W_{Map} \quad (15)$$

In this study, ($\Delta\eta_c$%) and (ΔW%) are obtained from Tables 1 and 2. ETASF and WASF are scaling factors of η_c and W respectively that are generated by the code, in relation to the standard compressor map embedded in the program.

The simple cycle configuration for the 226MW single shaft engine model with its components is depicted in Figure 13. This

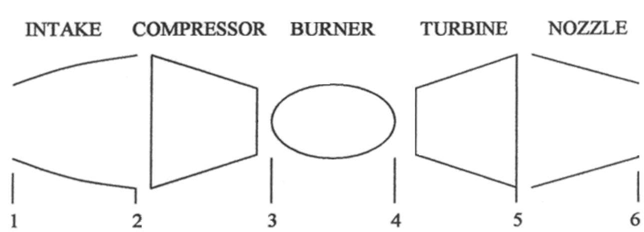

Figure 13 A simple gas turbine cycle [15]

figure also indicates input and output stations for each component, in which certain parameters are specified and components are linked. Some of the design point objectives are shown in Table 3.

Table 3 Engine model design point objective

Design Objective	Value
Mass Flow	620Kg/s
Pressure Ratio	16.6
Compressor Isentropic Efficiency	86%
Surge Margin	0.85
Burner Efficiency	99%
Turbine Inlet Temperature	1500K
Turbine Isentropic Efficiency	89%

The simulation is run under ISA conditions for a land based application. Under these conditions, the compressor maps of Figures 14 and 15 are plotted. These figures display axial compressor characteristics that would be expected in an actual compressor or any reasonably accurate model. An increase in mass flow influenced by an increase in shaft speed (N) leads to an increment in the pressure ratio as depicted in Figure 14. This means that more mechanical work is done to the air flow, leading to a higher compressor discharge pressure.

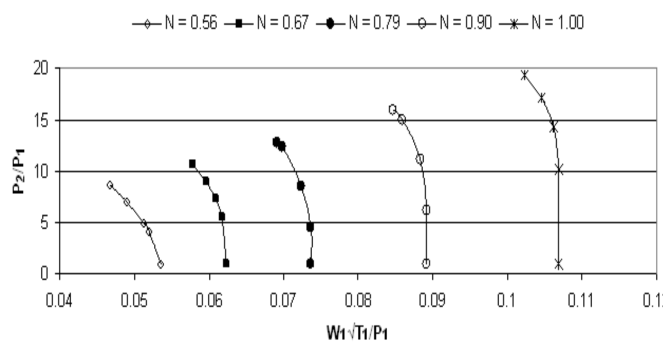

Figure 14 The compressor characteristics (pressure ratio and non-dim. mass flow)

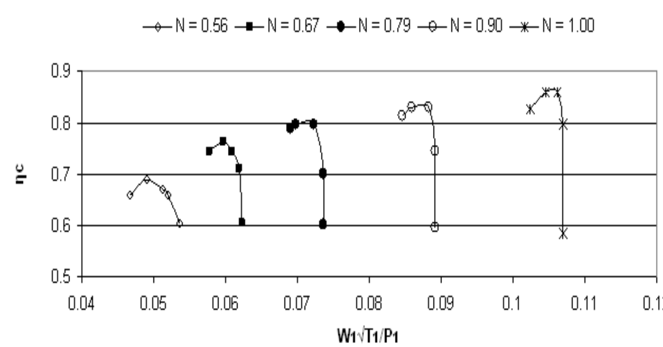

Figure 15 The compressor characteristics (compressor efficiency and non-dim. mass flow)

Figure 15 illustrates a corresponding increase in compressor efficiency at higher speed as a result of the higher compressor outlet pressure P_2. This is also inferred from equation (13).

The effects of fouling and washing on the compressor performance at the design point N = 1, is indicated in the subsequent figures. Figure 16 illustrates that when fouling occurs, air mass flow reduces as does engine speed. This is characterized by a shift in the speed line to the left, signifying an unattainable design speed.This figure also shows that for this shift of the equilibrium operating line, a reduction in the pressure ratio (more indicative on Table 4) would occur. What this means physically, is an increased loading on the blade due to fouling. More work is required to rotate the blade, thereby reducing the net power output. The washed compressor operating point indicated by the dotted line is seen to mitigate this effect, shifting towards the right and thereby improving the mass flow and pressure ratio.

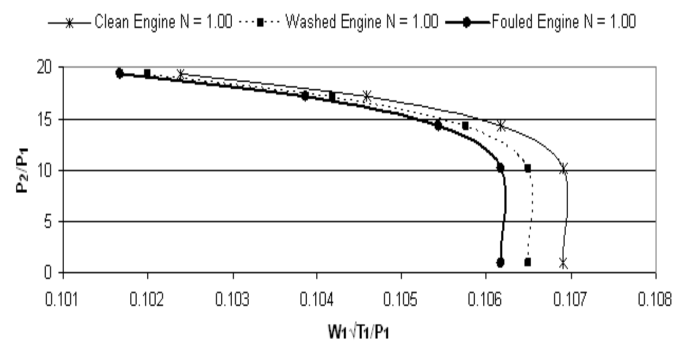

Figure 16 Pressure ratio versus non-dimensional mass flow for a clean, fouled and washed engine

Table 4 Pressure ratios for a clean, fouled and washed engine

	P_2/P_1	*Reduction/Increase*
Clean Engine	16.6	0.0%
Fouled Engine	16.52	0.48% ↓
Washed Engine	16.55	0.18% ↑

The relationship between the compressor efficiency and mass flow is emphasised for the cases of clean, fouled and washed engine provided in Figure 17. Similar to the previous figure, mass flow improvement in the washed engine translates to a better compressor efficiency influenced by pressure ratio increase. Another major benefit that can be conceived from this attempt to restore performance is the right shift, away from the hypothetical surge line.

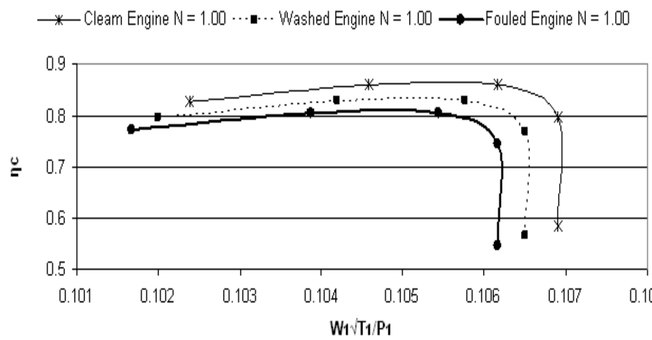

Figure 17 Compressor efficiency versus non-dimensional mass flow for a clean, fouled and washed engine

The evidence of a reduced power and thermal efficiency due to fouling, along with the corresponding gains due to washing is presented in Figures 18 and 19.

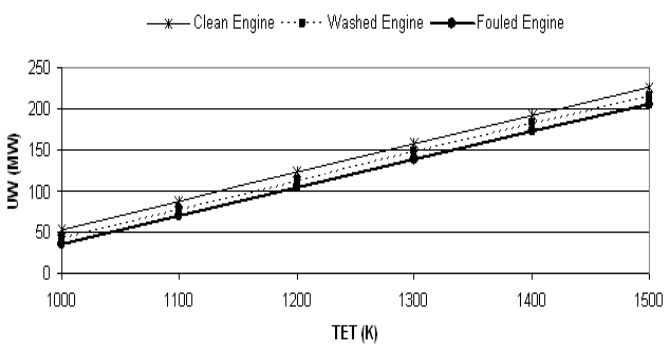

Figure 18 Power output versus turbine entry temperature for a clean, fouled and washed engine

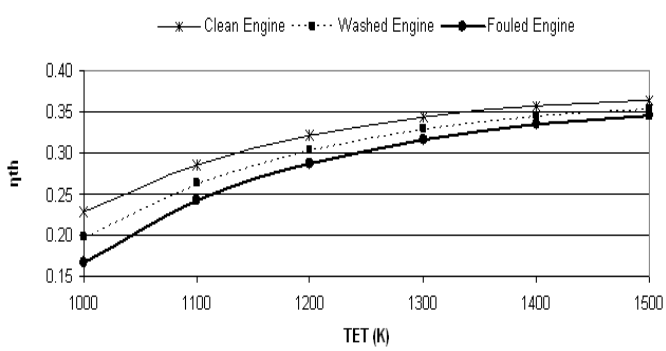

Figure 19 Thermal efficiency versus turbine entry temperature for a clean, fouled and washed engine

As expected, higher power output and thermal efficiency dominate at higher Turbine Entry Temperature (TET) due to a lower fuel required per unit of output (Specific Fuel Consumption – SFC) at higher TET.

The plot of power output against TET indicates 8.7% reduction of the design power due to fouling and 4.4% increase due to washing at 1500K. This recovery amounts to an additional 50% of the lost power. Similarly, the thermal efficiency reduces by 5.3% and increases by 2.5% due to fouling and washing respectively. These gains are attributed to better supply in the quality of air; enhanced mass flow as blade passage area increases, in addition to better compressor delivery pressure proven from Table 4.

Another point of observation during the investigation is that at the constant TET, the fuel flow demand is greater in a clean engine than the degraded and washed engine (see Figure 20). A similar account is reported in Kurz and Brun [16] which states that due to reduced compressor efficiency, the compressor exit temperature is greater, leading to a reduced fuel flow. This explanation is valid for the Compressor Discharge Temperatures (CDT) obtained; 689K, 715K and 702K (for clean, fouled and washed engine respectively).

It is imperative to note from equation (16), that CDT is affected by pressure ratio as well. A reduced pressure ratio reduces the CDT due to lesser compression of air. This is an opposing effect to the accompanied compressor efficiency reduction that increases CDT. From the previous findings, it hence suggests that the drop in CDT due to compressor efficiency reduction is more significant than its compensating increase due to pressure ratio decrease.

$$CDT = CIT\left[1+\frac{1}{\eta_c}\left(PR^{\left(\frac{\gamma-1}{\gamma}\right)}-1\right)\right] \qquad (16)$$

The percentage reduction of fuel flow for the range of TET is shown in Figure 20. This signifies 3.6% and 1.9% reduction of fuel flow for the fouled and washed engines respectively at design point TET = 1500K. It is also important to mention from an economic point of view that the accumulated cost of power loss in earnings and availability due to fouling is likely to outweigh the cost of fuel flow reduction in the fouled engine.

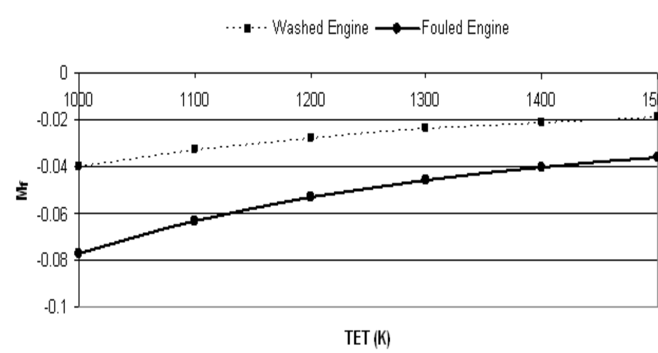

Figure 20 Fuel flow reduction for a fouled and washed engine

CONCLUSIONS

The results present an optimistic case of washing, indicating 50% recovery of the lost power. Though most of the physical removal of the particles is seen at the leading edge, these findings validate the experimental results of Gbadebo et al [17] claiming the leading edge is the most sensitive part of the blade.

It is observed that the assumption of equal stage polytropic efficiencies to calculate isentropic efficiency is more applicable to clean engine condition. This approach does not account for variation in the levels of fouling in compressor stages, which often lead to more work being done by the next stages (preheat effect). In addition to that, the reduced effectiveness of washing at rare stages is not taken into consideration. A stage-by-stage approach with empirical data may provide a rather more precise estimation of the isentropic efficiency, but it is a very length process. However, in principle the front stages are found to be most fouled and on-line compressor washing is known to be more effective in these early stages.

It is nevertheless worthy of note from this study that on-line compressor cleaning;

- improves the power output and consequently thermal efficiency of the gas turbine engine
- ensures a safer operation away from the surge line with good utilization of shaft speed leading to an enhanced mass flow and pressure ratio.

This investigation points out two key outcomes of on-line washing, which are; retarding the reduction in performance due to fouling and enhancing power loss recovery. While they may be constraints on how much can be recovered (the latter), there is more assurance on the former. The major advantage then lies in the proactive and preventive loss of power which can be obtained by an early implementation of a regular wash. In an ideal case it would be from the onset of engine commissioning.

ACKNOWLEDGMENTS

The authors owe gratitude to R-MC Power Recovery Ltd for their continuing technical support and funding. The opinions expressed here are those of the authors and not necessarily those of R-MC.

NOMENCLATURE

c	blade chord
C_D	drag coefficient
C_{Da}	annulus drag coefficient
C_{Dp}	profile drag coefficient
C_{Ds}	drag coefficient for secondary losses
CDT	compressor discharge temperature
CIT	compressor inlet temperature
c_p	specific heat at constant pressure
C_L	lift coefficient
ETASF	compressor efficiency scaling factor
h	blade height (span)
ΔH	enthalpy change
ISA	international standard atmosphere
k	roughness height
K	kelvin
LE	leading edge
M_f	fuel mass flow
N	Shaft or rotor speed
NOx	nitrogen oxide
OEM	original equipment manufacturer
P	total pressure
pbns	pressure based navier stokes
P_s	static pressure
PR	pressure ratio
s	blade pitch
ske	standard k-epsilon
SFC	specific fuel consumption
T	total temperature
T_s	static temperature
TET	turbine entry temperature
TP	trailing passage or pitch
μm	micrometer
U	blade speed
UW	power or work output
V	velocity
W	non-dimensional air mass flow
WASF	non-dimensional mass flow scaling factor
WR	wake region

Symbols

α	air flow angle
β	blade metal angle
λ	work done factor
ϕ	flow coefficient
ψ	stage loading coefficient
η	efficiency
ρ	air density
Δ	change
ω	blade profile total pressure loss coefficient
γ	specific heat ratio

Subscripts

0	stagnation
1	rotor inlet, cascade inlet
2	rotor outlet, cascade outlet
3	stator inlet
4	stator outlet
a	axial, annulus
amb	ambient

c	isentropic
m	mean
Map	map
th	thermal
p	polytropic
tot	total

REFERENCES

[1] Meher-Homji C.B. and Bromley A. F., 2004, "Gas Turbine Axial Compressor Fouling and Washing", Proceedings of the 33rd Turbomachinery Symposium, pp 165 – 191.

[2] Stalder, J.P., 2001, "Gas Turbine Compressor Washing State of the Art Field Experiences", ASME Transactions, Journal of Engineering for Gas Turbines and Power, 123, pp 363-370.

[3] Syverud, E. and Bakken, L.E., 2003, "Gas Turbine Operation Offshore; On-line Compressor Wash at Peak Load", Proceedings of ASME Turbo Expo, Power for Land, Sea and Air, Atlanta, Georgia, USA.

[4] Boyce, M.P. and Gonzalez, F., 2007, "A Study of Online and Online Turbine Washing to Optimize the Operation of a Gas Turbine", ASME Transactions, Journal of Engineering for Gas Turbine and Power, 129, pp 114-122.

[5] Thames, J.M., Stegmaier, J.W and Ford, J.J., Jr., 1989, "On-line Compressor Washing Practices and Benefits", In Gas Turbine and Aeroengine Congress Exposition, Toronto, Canada, 89-GT-91.

[6] Dixon, S.L., 1998, "Fluid Mechanics and Thermodynamics of Turbomachinery", Butterworth-Heinemann. U.S.A.

[7] Pollard D. and Gostelow J., 1967, "Some Experiments at Low Speed on Compressor Cascades", ASME Transactions, Journal of Engineering for Power, 88-89, pp. 427-436.

[8] Lieblein, S., Roudebush, W.H., 1956, "Theoretical Loss Relation for Low Speed Two Dimensional Cascade Flow", NACA Technical Note 3662, Lewis Flight Laboratory, Cleveland, Ohio.

[9] Sawyer, J. W., 1980, "The Aerodynamic Design of Axial-Flow and Centrifugal Compressors", Chapter 3, Sawyer's Gas Turbine Engineering Handbook.

[10] Amaral, C.D., Guerra, V.G., Arouca, F.O., Coury, J.R., 2010, "Effect of the Salt Solution Concentration in the Number and Size Distribution of Atomized Nanometric Aerosol Particles", Materials Science Forum, 660 – 661, pp 581 – 586.

[11] Mund, F.C., 2006, "Coordinated Application of CFD and Gas Turbine Performance Methods", PhD thesis, Cranfield University, U.K.

[12] Howell, A. R., 1945, "Fluid Dynamics of Axial Compressors", Proceedings of the Institution of Mechanical Engineers", 153, pp. 441-452.

[13] Horlock, H. J., 1973, "Axial Flow Compressors: Fluid Mechanics and Thermodynamics", Robert E. Publishing Co., Inc., Huntington, New York.

[14] Howell, A. R. and Bonham, R.P., 1950, Overall and Stage Characteristics of Axial-Flow Compressors, Proceedings of the Institution of Mechanical Engineers, 163, pp. 235-248.

[15] Pachidis, V., 2009, "Gas Turbine Performance Simulation", Thermal Power MSc Course Notes, Cranfield University, U.K.

[16] Kurz, R. and Brun, K., "Gas Turbine Tutorial -Maintenance and Operating Practices Effects on Degradation and Life", pp 173 -185.

[17] Gbadebo, S.A. and Cumpsty, N.A., 2004, "Influence of Surface Roughness on Three-Dimensional Separation in Axial", ASME Transactions, Journal of Turbomachinery, 126, pp. 455 - 463.